ACS SENSORS

pubs.acs.org/acssensors

Article

TADF-Emitting Zn(II)-Benzoporphyrin: An Indicator for Simultaneous Sensing of Oxygen and Temperature

Silvia E. Zieger,[§] Andreas Steinegger,[§] Ingo Klimant, and Sergey M. Borisov*

Cite This: *ACS Sens.* 2020, 5, 1020−1027

Read Online

ACCESS | Metrics & More | Article Recommendations | Supporting Information

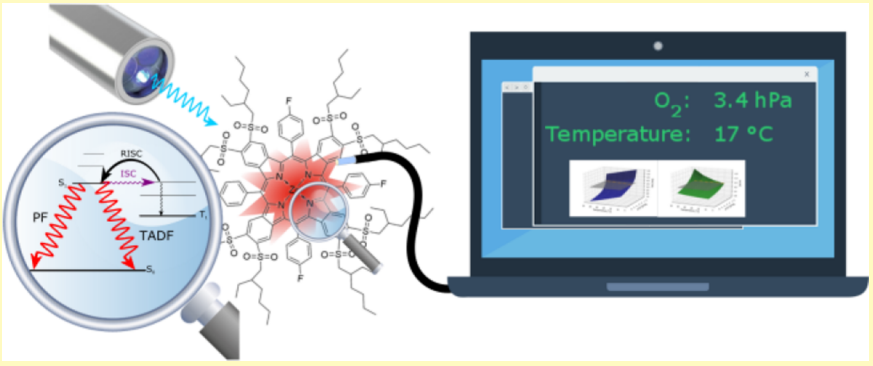

ABSTRACT: A new luminescent indicator is presented that enables simultaneous measurement of oxygen and temperature at a single wavelength. The indicator, an alkylsulfone-substituted Zn(II)-*meso*-tetraphenyltetrabenzoporphyrin, emits prompt and thermally activated delayed fluorescence (TADF). TADF is sensitive toward oxygen and temperature and is referenced against prompt fluorescence (PF) that is not affected by oxygen. The information on both parameters is accessed from the decay time of TADF and the temperature-dependent ratio of TADF and PF. Sensor foils, made from poly(styrene-*co*-acrylonitrile) and the indicator dye, enable temperature-compensated trace oxygen sensing (0.002−6 hPa pO_2) at ambient conditions. Compared to the previously reported dual sensors based on two emitters, the new sensor significantly simplifies the experimental setup and eliminates risks of different leaching or photobleaching rates by utilizing only one indicator dye and operating at a single wavelength.

KEYWORDS: *optical oxygen sensing, dual sensor, temperature compensation, molecular thermometer, fluorescence*

Optical oxygen sensors utilize luminescent indicators such as metalloporphyrins[1−11] or Ru(II)−polypyridyl complexes[12,13] and others[14,15] embedded in oxygen-permeable matrices.[16,17] Like any chemosensor, optical oxygen sensors are always affected by temperature.[16,17] This cross-talk, however, can be corrected if temperature is measured. This can be done with help of a conventional thermometer or using an optical temperature probe.[1−3,15,18−54] The latter rely on oxygen-insensitive luminophores such as inorganic phosphors,[7,10,13] quantum dots,[3,55] or metal−organic indicators such as Eu(III)-*β*-diketonate complexes.[2,4,6,12,31] Temperature indicators with pronounced cross-talk to oxygen such as Ru(II)−polypyridyl complexes[1,5,11] have to be incorporated in gas-impermeable matrices such as polyacrylonitrile.[15]

Dual sensors for oxygen and temperature[1−13,15,31,55] are particularly interesting because they allow compensation of the temperature effects at exactly the same place. This is essential in systems with strong temperature gradients. Moreover, this is the only format suitable for simultaneous imaging of both parameters, for example, for application as pressure-sensitive paints.[2,13,15,22] In all these systems, the signal from the temperature probe has to be separated from the oxygen signal either spectrally or temporally. Although systems based on two indicators with largely different decay times have been reported,[4,13] spectral separation is by far the most popular strategy.[3,5,6,8,9,11,15,31,55] Mostly combinations of metalloporphyrins or Ru(II)−polypyridyl complexes[12,13] with temperature probes, including inorganic phosphors,[7,10,13] quantum dots,[3,55] or metal−organic indicators such as Eu(III)-*β*-diketonate complexes[2,4,6,12,31] have been explored. The main disadvantages of the multiprobe approach include higher complexity in material chemistry, drifts because of different leaching and photobleaching rates, and complex optical setups. As one possibility, the complexity of such systems can be reduced by finding a single indicator, which can give spectrally or temporally distinct responses on temperature and on

Received: December 19, 2019
Accepted: March 27, 2020
Published: March 27, 2020

https://dx.doi.org/10.1021/acssensors.9b02512
ACS Sens. 2020, 5, 1020−1027

oxygen. Unfortunately, indicators with such properties are extremely rare.

In particular, indicators based on thermally activated delayed fluorescence (further referred to as DF), can be promising for the temperature-compensated determination of oxygen because DF is inherently sensitive toward temperature.[48,49,56,57] A plethora of DF emitters have emerged in research for the organic light-emitting diode industry.[58−60] Most of these dyes, however, have photophysical properties unsuitable for optical sensing. They usually have poor molar absorption coefficients resulting in reduced brightness and absorb in the UV to blue parts of the electromagnetic spectrum. We have previously shown that some electron-deficient Pt(II) and Pd(II)-benzoporphyrins simultaneously display fairly bright DF and phosphorescence.[57] The singlet−triplet energy gap decreased and the DF quantum yield increased with increasing electron withdrawing character of substituents in the β-position of the porphyrin. The emission of these complexes is dually responsive to oxygen (decay time change) and temperature (a ratio of DF to phosphorescence) and allows determination of both parameters via two-wavelength read-out. We thus envisioned that similar benzoporphyrins could be used to collect the same information via single-wavelength read-out providing that they simultaneously emit prompt fluorescence (PF) and DF because these two emission types are spectrally identical. By using a multifrequency phase fluorometry method, both temperature and oxygen can be determined from the DF with the PF serving as an intrinsic reference.

Herein, we present a dually sensitive material relying on a red-emitting Zn(II)-benzoporphyrin that features both PF and DF. The new material enables simultaneous sensing of oxygen and temperature with a simple optical setup (one emission channel) with frequency domain read-out at two different modulation frequencies.

EXPERIMENTAL SECTION

Details about materials, instrumentation, NMR, and MS spectra are provided in the Supporting Information.

Preparation of the Indicator Dye Zn-OS. The ligand *meso*-tetra(4-fluorophenyl)-tetra(4,5-bis(2-ethylhexylsulfonyl))-benzoporphyrin (H_2-OS) was prepared according to the literature.[57]

Zn(II) *meso*-tetra(4-fluorophenyl)-tetra(4,5-bis(2-ethylhexylsulfonyl))-benzoporphyrin (Zn-OS): 30 mg (13 μmol, 1 eq) of the ligand H_2-OS was dissolved in a mixture of dichloromethane and methanol (10 mL, CH_2Cl_2/MeOH 4:1 v/v). In total, 573 mg of zinc acetate dihydrate (2.61 mmol, 200 equiv) and 21 mg of sodium acetate (261 μmol, 20 equiv) were added to the reaction mixture, and the solution was stirred for 5 min. Turnover was monitored via UV−vis spectroscopy. After quantitative conversion, the reaction mixture was washed with distilled water (4 × 20 mL). The organic layer was dried over Na_2SO_4, and the solvent was removed under reduced pressure resulting in dark green powder (24 mg, yield 80%). UV−vis: $\lambda_{max}/\varepsilon$ (nm/M^{-1} cm^{-1}) in toluene: 490/386.000, 623/28.000, 664/79.000.

^{1}H NMR (300 MHz, $CDCl_3$) δ in ppm: 8.16 (s, 16H), 7.68 (m, 8H), 3.47 (m, 16H), 1.95 (m, 8H), 1.48−1.34 (m, 32H), 1.28−1.21 (m, 32H), 0.84 (m, 48H).

^{13}C NMR (76 MHz, $CDCl_3$) δ in ppm: 166.69, 163.34, 144.27, 140.52, 137.21, 136.28, 134.81, 130.29, 119.28, 117.59, 117.30, 60.35, 34.56, 32.72, 28.22, 26.03, 22.87, 14.15, 10.32.

HRMS (MALDI-TOF): calcd for $C_{124}H_{160}F4N_4O_{16}S_8Zn$ $[M + H]^+$, 2358.884; found, 2358.905.

Sensor Preparation. Poly(styrene-*co*-acrylonitrile) [PSAN, acrylonitrile 30 wt %, Aldrich, MW = 185.00 (GPC)] and dye Zn-OS (1 wt % with respect to PSAN) were dissolved in chloroform (7.5 wt % dye + PSAN in chloroform), and the solution was knife-coated (a 25 μm thick wet film) onto dust-free poly(ethylene terephthalate) (PET) support foils [125 μm biaxially oriented PET foils (MELINEX 506) supplied by Pütz GmbH Co. Folien KG (www.puetz-folien.com)]. After evaporation of the solvent, the sensor foils were dried at 60 °C for 24 h.

Measurements. Luminescence measurements were conducted in the gas phase at different temperatures (10−41 °C). A sensor spot, prepared by punching the planar foil, was incorporated into a glass capillary, which was then deployed into a cryostat from Avantor [model 1150S (us.vwr.com)] for temperature control. Inlets and outlets of the capillary were connected to stainless steel gas pipes using a Tygon R-3603 tube, and the gas pipes were also placed into the cryostat. The inlet of the gas pipe was further connected to a gas-mixing device based on two mass flow controllers (Voegtlin red-y smart series; www.voegtlin.com). A custom-made software was used to adjust the oxygen partial pressure for calibration by mixing nitrogen (99.999% purity) and a test gas (2.00 vol % in nitrogen), obtained from Linde (www.linde-gas.at). The gas flow was 200 mL/min. The overall luminescence phase shifts and overall luminescence amplitudes (from PF and DF, c.f. Supporting Information section Data Analysis) were measured with a lock-in amplifier (SR830 DSP, Stanford Research, www.thinksrs.com). The excitation of the sensor material was performed with a 490 nm light-emitting diode (LED) from Roithner (www.roithner-laser.com). The LED light was filtered through a combination of a BG 12 glass filter and a "Lagoon-blue" plastic filter obtained from bk Interferenzoptik (www.interferenzoptik.de) and LEE Filters (www.lee-filters.com), respectively. A bifurcated fiber bundle was used to guide the excitation light to the sensor spot and to transfer the emitted luminescence to the detector (photomultiplier H9306-02 from Hamamatsu, www.sales.hamamatsu.com). A combination of a RG 645 long-pass filter obtained from bk Interferenzoptik and a plastic filter "Primary Red" from LEE Filters was used in front of the photomultiplier. A solution of fluorescent Lumogen orange (Kremer Pigmente, www.kremer-pigmente.com) was used as a 0 phase standard. For calibration cycles, pO_2 was adjusted between 0 and 6 hPa at one temperature and at one modulation frequency (19 or 61 Hz). After the measurement at the second modulation frequency, the whole cycle was completed two more times. This was done for each temperature. Additionally, the luminescence decay times and intensities were measured for the sensor foil submerged in the anoxic aqueous solution of sodium sulphite (2% wt) containing catalytic amounts of $CoCl_2$. Discrepancy between the values obtained in the sodium sulfite solution and in the gas phase with nominal pO_2 of 0 hPa indicated contamination of the gas phase with traces of oxygen. It was corrected, as described in detail in the Supporting Information.

The limit of detection (LOD) was estimated using the blank value method (blank value + 3 × standard deviation).

Data Analysis. The evaluation of the luminescence phase shift was done based on the variation of the dual lifetime reference technique using the following equation:[61]

$$\tau = \frac{f_1^2 - f_2^2 \pm \sqrt{(f_2^2 - f_1^2)^2 - 4(f_1^2 f_2 \cot(\Phi_2) - f_1 f_2^2 \cot(\Phi_1))\cdot(f_2 \cot(\Phi_2) - f_1 \cot(\Phi_1))}}{4\pi(f_1^2 f_2 \cot(\Phi_2) - f_1 f_2^2 \cot(\Phi_1))} \quad (1)$$

where Φ_1 and Φ_2 are the overall luminescence phase shifts at the

https://dx.doi.org/10.1021/acssensors.9b02512
ACS Sens. 2020, 5, 1020−1027

modulation frequencies f_1 = 19 Hz and f_2 = 61 Hz, respectively. The calculated luminescence lifetime τ has to be interpreted as an apparent lifetime, which deviates from the lifetime determined by other methods (time domain) as some assumptions seem to be violated when using phase-fluorometry.[62] However, the system is still intrinsically referenced and can be recalibrated for each measurement adjustment with four calibration points.[63]

The intensity ratio of PF and DF was calculated according to the following equation

$$\frac{I_{PF}}{I_{DF}} = \frac{\omega\cdot\tau - \tan(\Phi)}{(1 + (\omega\cdot\tau)^2)\cdot\tan(\Phi)}, \qquad \omega = 2\cdot\pi\cdot f \tag{2}$$

where Φ is the overall luminescence phase shift at the corresponding modulation frequencies f_1 or f_2, and τ is the apparent lifetime of the indicator at given temperature and oxygen partial pressure, respectively. For further explanations and the derivation of eq 2, please refer to the Supporting Information. As the chosen modulation frequencies are low, the measurement of luminescence phase shifts can suffer from electromagnetic interferences. The estimation of the error propagation is crucial for appropriate data evaluation. Thus, an outlier test was applied to the measurement data before processing the fitting, and each time, the average value and the standard deviation were determined for both the apparent lifetime and the intensity ratio. The fitting of the apparent lifetime was performed in two dimensions. The Stern−Volmer two-site model[22,64,65] was used to fit the dual response of the lifetime because of oxygen quenching, whereas a linear regression was used for temperature dependency. The final fit model for the apparent lifetime can be summarized as

$$\frac{\tau}{\tau_0(T)} = \frac{f(T)}{1 + K_{sv,1}(T)\cdot pO_2} + \frac{1 - f(T)}{1 + K_{sv,2}(T)\cdot pO_2} \tag{3}$$

where τ and $\tau_0(T)$ are the apparent lifetimes in the presence and absence of oxygen, respectively, $f(T)$ and $(1 - f(T))$ represent the quenchable and the less-quenchable parts of the luminescence, respectively, and $K_{sv,1}(T)$ and $K_{sv,2}(T)$ are the Stern−Volmer constants for the quenchable and less-quenchable parts of luminescence, respectively. Each of the parameters is given at a certain temperature.

In contrast to the fitting of the apparent lifetime, the fit model for the intensity ratio is based on empirical studies and was selected according to the minimal chi-square value χ^2. The best result with a chi-square χ^2 of 1.73×10^{-3} was obtained using a reciprocal quadratic function for the oxygen response combined with a linear regression for the temperature response. The overall fit function is shown below.

$$\frac{I_{DF}}{I_{PF}} = \frac{1}{a(T)\cdot pO_2^{\,2} + b(T)\cdot pO_2 + c(T)} \tag{4}$$

where a, b, and c are numerical coefficients.

Based on these fitting models, the sensor can be recalibrated using two calibration points for both parameters.

RESULTS AND DISCUSSION

Indicator Dye. Pt(II) and Pd(II)-tetrabenzoporphyrins are popular phosphorescent oxygen indicators. They display high molar absorption coefficients, NIR emission, and good stability. Alkylsulfone-substituted Pt(II) and Pd(II) *meso*-tetraphenyltetrabenzoporphyrins have comparably efficient DF in addition to the typical phosphorescence of Pt(II) and Pd(II) porphyrins.[57] DF is a strongly temperature-dependent process. In contrast to PF and phosphorescence that are quenched at higher temperatures because of the more efficient nonradiative deactivation, the intensity of DF initially increases with temperature. Consequently, this effect can be used for temperature measurement. For the simultaneous determination of temperature and oxygen, the indicator is required to have spectrally or temporally distinct responses on temperature and on oxygen. For the alkylsulfone-substituted Pt(II) and Pd(II) *meso*-tetraphenyltetrabenzoporphyrins, the temperature can be accessed via the ratio of DF and phosphorescence. Additionally, the oxygen concentration can be determined via the luminescent decay time of either phosphorescence or DF because the excited triplet state of the dye is efficiently quenched by molecular oxygen. For this system, temperature measurement requires two-wavelength read-out.

Compared to ratiometric measurement, single-wavelength read-out can further reduce the complexity of the measurement setup. In contrast to DF and phosphorescence, DF and PF emit at the same wavelength and hence would allow single-wavelength read-out. The Pt(II) and Pd(II) *meso*-tetraphenyltetrabenzoporphyrins are therefore unsuitable for this read-out because a strong heavy atom effect results in the very efficient population of the triplet state, thus leading to the absence of PF. Therefore, in order to change the type of the emission in the alkylsulfone-substituted *meso*-tetraphenyltetrabenzoporphyrin complexes, we used Zn(II) as a central atom instead of Pt(II) or Pd(II). The Zn(II)-alkylsulfone-substituted *meso*-tetraphenyltetrabenzoporphyrin (Zn-OS, Figure 1), however, retains the small singlet−triplet energy gap

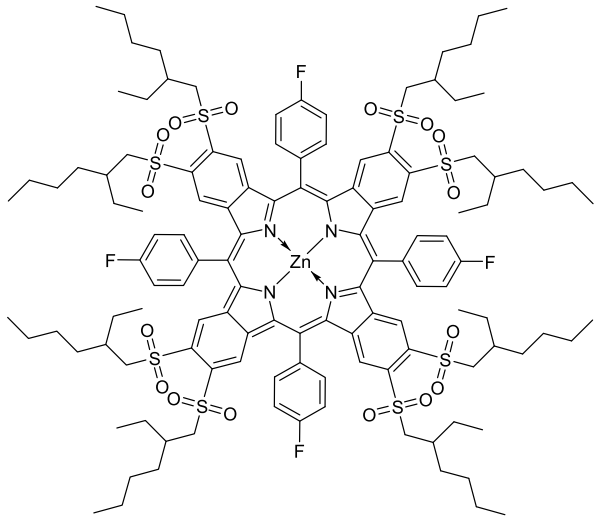

Figure 1. Chemical structure of Zn-OS.

that enables DF. The singlet−triplet energy gap estimated from temperature dependency of the DF decay time using an Arrhenius type model is ~1646 cm^{-1} (Supporting Information, Figure S6 and eq S12).[19]

Photophysical Properties of the Indicator Dye. The dye efficiently absorbs in the blue to green (porphyrin Soret band, 490 nm) and red part (Q bands, 623 and 664 nm) of the spectrum (Figure 2). The molar absorption coefficients are exceptionally high (Table 1), particularly for the Soret band. The emission is located in the red to far-red region (λ_{max} 667 nm). Although the Stokes shift (λ_{max} in the Q band−λ_{max}em) is very small (3 nm), excitation in the Soret band (λ_{max} 490 nm) allows excellent separation of the emission from the excitation ($\Delta\lambda$ = 177 nm) which is highly valuable for sensing applications.

The emission can be attributed to the combination of PF and DF; no phosphorescence is observed for the Zn(II) porphyrin. For the dye in toluene solution, ensuring complete deoxygenation of solutions is very challenging; hence, it was not possible to reliably determine the overall quantum yield

https://dx.doi.org/10.1021/acssensors.9b02512
ACS Sens. 2020, 5, 1020−1027

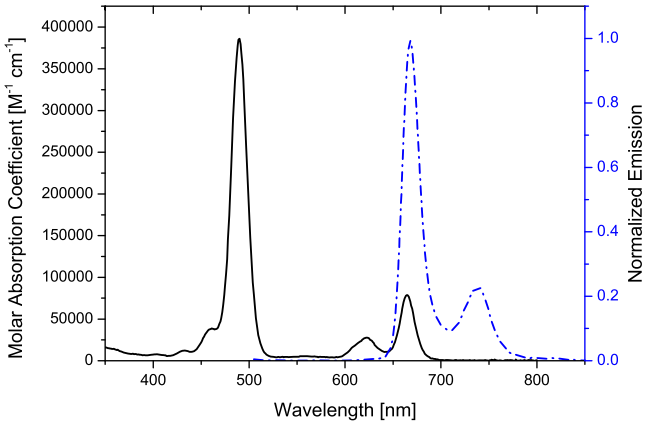

Figure 2. Absorption (solid black line) and emission (dashed blue line) spectra of Zn-OS in toluene at 25 °C.

Table 1. Photophysical Properties of Zn-OS Dissolved in Toluene and Immobilized in PSAN at 25 °C[b]

matrix	λ_{abs}max [nm]/ε [m^{-1} cm^{-1}]	λ_{em}max [nm]	τ_{DF} [ms]	ϕ [%]
Toluene	490/386.000, 623/28.000, 664/79.000	667	≥1	n.d.
PSAN	495, 628, 671	675	7.87[a]	2.4 PF, 0.9 DF[a]

[a]Under anoxic conditions (2 wt % aqueous sodium sulphite solution). [b]n.d.—not determined.

and DF lifetime. In fact, DF lifetime exceeds 1 ms, which results in extremely efficient quenching by molecular oxygen. On the other hand, for the dye immobilized in PSAN, anoxic conditions can easily be achieved by immerging the foil into the aqueous sodium sulphite solution.

At 25 °C, the overall quantum yield is moderate (3.3%) with roughly 30% contribution of DF and 70% of PF (Table 1). Yet, the brightness is acceptably high because of the high molar absorption coefficient. At room temperature, the DF decay time is around 8 ms making the indicator suitable for oxygen trace sensors.

Sensing Materials. The choice of the polymer is an essential part in preparation of sensing materials based on immobilized indicators. The long luminescent lifetime of Zn-OS requires polymers with moderate to low oxygen permeability even for trace oxygen sensors. Therefore, a copolymer of moderately oxygen-permeable polystyrene and virtually gas-impermeable poly(acrylonitrile) was selected. PSAN containing 30 wt % acrylonitrile was used. PSAN with 39 wt % acrylonitrile has an oxygen permeability coefficient (P) of 0.35 × 10^{-13} cm^3 (STP) cm cm^{-2} s^{-1} Pa^{-1},[66] which is significantly lower than for polystyrene [P = 2.0× 10^{-13} cm^3 (STP) cm cm^{-2} s^{-1} Pa^{-1}].[66] Because the material based on combination of Zn-OS and PSAN is still highly sensitive to oxygen, its response was studied in the range from 0 to 6 hPa pO_2.

Response of Zn-OS/PSAN to Oxygen and Temperature. Oxygen and temperature affect the photophysical properties of Zn-OS but in a different way, making possible simultaneous sensing of the two parameters with a single indicator. Importantly, the intensity of PF (I_{PF}) is neither significantly affected by temperature nor by molecular oxygen and thus can be utilized as an intrinsic reference. Dynamic quenching by oxygen results in decrease of the DF decay time (increase of τ_0/τ) and the intensity I_{DF} (Figure 3B,D). As expected from the long decay time of the DF, the quenching is very efficient. The LOD at 26 °C was estimated to be 0.002 hPa.

In agreement with the behavior of most optical oxygen sensors, dynamic quenching becomes more efficient as the temperature is increased (Figure S7). On the other hand, whereas the DF lifetime decreases with temperature as well (Figure 3A), DF is enhanced with increasing temperature (Figure 3C) because more molecules have the necessary energy for the reverse intersystem crossing. The temperature and oxygen effects on luminescent properties of the Zn-OS are summarized in Table 2.

The influence of temperature and oxygen on the luminescence decay curves is shown in Figures S8 and S9. In these graphs, the intensity at the plateau is the sum of PF and DF. The first point of the decay represents the intensity of the DF. The ratio $I_{DF}/_{PF}$ changes the relative positions of the

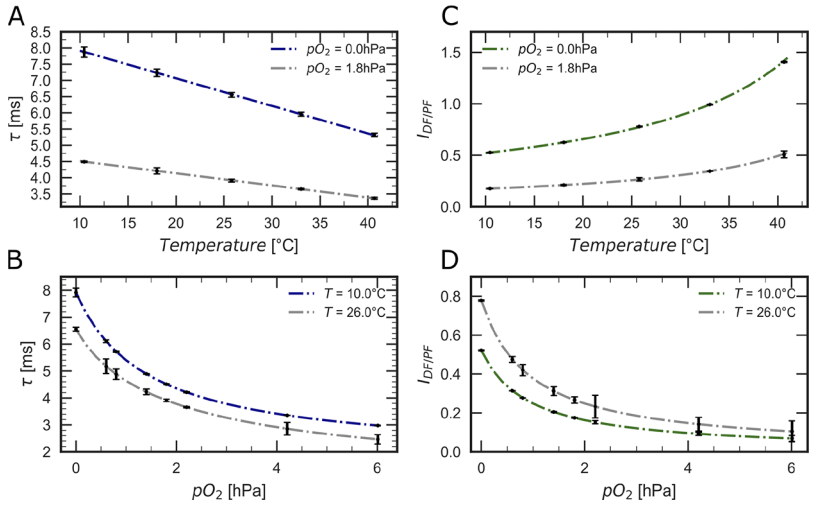

Figure 3. Response of the apparent luminescence decay time τ (A,B) and the intensity ratio ($I_{DF}/_{PF}$) (C,D) for the dual sensor to temperature (A,C) and oxygen (B,D). The response is exemplified for two different temperatures and oxygen partial pressures. The fit (indicated by dash-dot lines) is performed according to eqs 3 and 4.

https://dx.doi.org/10.1021/acssensors.9b02512
ACS Sens. 2020, 5, 1020−1027

Table 2. Summary of the Effects of Oxygen and Temperature on Luminescence Properties of Zn-OS

parameter	oxygen ↑	temperature ↑
I_{PF}	no effect	no pronounced effect
I_{DF}	↓	↑
τ_{DF}	↓	↓

plateau and the first point of the decay curve. Changes in decay time are manifested in different slopes of the decay curves.

Dual Sensing of Oxygen and Temperature. For the isolation of both parameters (τ and $I_{DF}/_{PF}$) from single-wavelength read-out, a multifrequency phase fluorometry method was used (Data Analysis section). The experimental data form calibration planes (Figure 4A,B) that can be fitted according to eqs 3 and 4 for both the apparent lifetime (τ or

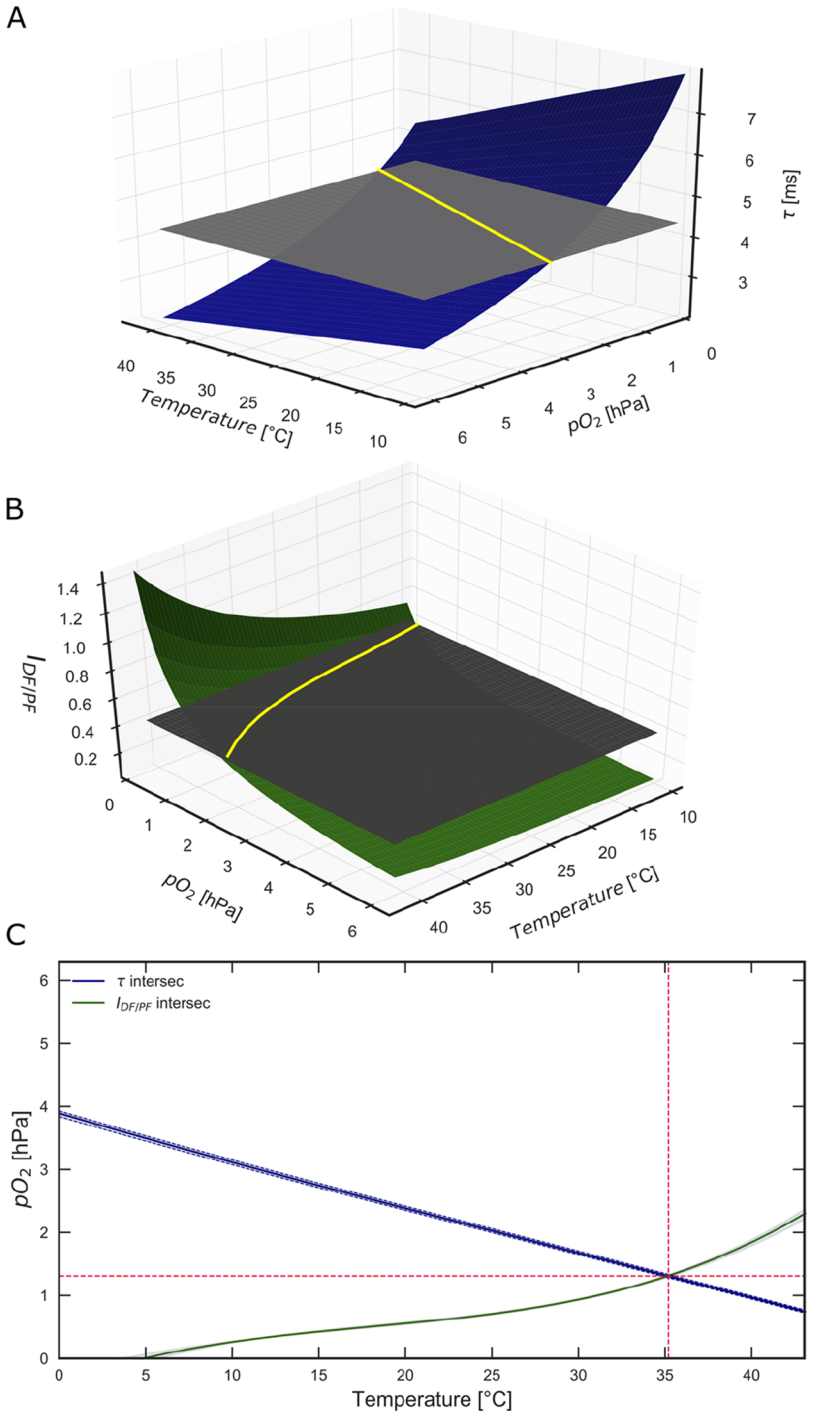

Figure 4. Luminescence response of the Zn-OS/PSAN material to temperature and oxygen and illustration of the data analysis using analytical geometry. (A,B) Calibration planes (colored surfaces representing the mean values at each point) for the apparent luminescence decay time and the intensity ratio (delayed I_{DF} vs prompt I_{PF} luminescence). Horizontal gray planes exemplify the τ and $I_{DF}/_{PF}$ obtained at given conditions. Curves resulting from the intersection of the calibration planes and horizontal gray planes are shown in yellow color. (C) Intersection curves (A,B) with the intercept point indicating the unique pair of temperature and pO_2 values.

https://dx.doi.org/10.1021/acssensors.9b02512
ACS Sens. 2020, 5, 1020−1027

τ_0/τ) and the intensity ratio ($I_{DF}/_{PF}$). In each case, the fitting reveals a continuous and monotonous calibration plane, which is the basic prerequisite for definite analysis of the sample data.

The analysis of the sample data is then conducted in the Euclidean space using analytical geometry. Upon determination of the current parameters (τ or τ_0/τ and $I_{DF}/_{PF}$) according to eqs 1 and 2, a horizontal sample plane is generated for each parameter (gray planes, as shown in Figure 4A,B). The horizontal plane is then crossed with the calibration plane for the given parameter to determine the intersection curves (yellow lines, as shown in Figure 4A,B). The intersection curves consist of pairs of temperature and oxygen that result in the given parameter (Figure 4C). Subsequently, the intercept of the intersection curves reveals the actual temperature and the oxygen partial pressure of the sample, which are clearly defined because of a continuous and monotonous calibration plane (Figure 4C).

CONCLUSIONS

We have presented an alkylsulfone-substituted Zn(II)-*meso*-tetraphenyltetrabenzoporphyrin that simultaneously exhibits PF and DF. Although the luminescence quantum yields are moderate, the overall brightness is good because of very high molar absorption coefficients. Additionally, the excitation and the emission are well separated, as the excitation is performed in the Soret band of the indicator. This allows the utilization of the full emission peak/brightness of the indicator. The combination of PF and DF enables simultaneous determination of oxygen and temperature using a multifrequency phase fluorometry method. Importantly, this is done using a single indicator and a single-wavelength readout. This simplifies the experimental setup and does not bear risks of different leaching or photobleaching rates that may compromise the performance of the mutiparameter sensors based on combination of two indicators.

ASSOCIATED CONTENT

Supporting Information

The Supporting Information is available free of charge at https://pubs.acs.org/doi/10.1021/acssensors.9b02512.

NMR and MS spectra of indicator and additional information on data processing algorithms (PDF)

AUTHOR INFORMATION

Corresponding Author

Sergey M. Borisov − *Institute of Analytical Chemistry and Food Chemistry, Graz University of Technology, 8010 Graz, Austria;* orcid.org/0000-0001-9318-8273; Phone: +43 (316) 873 32516; Email: sergey.borisov@tugraz.at

Authors

Silvia E. Zieger − *Institute of Analytical Chemistry and Food Chemistry, Graz University of Technology, 8010 Graz, Austria; Department of Biology, Aarhus University Centre for Water Technology (WATEC), 8000 Aarhus C, Denmark*

Andreas Steinegger − *Institute of Analytical Chemistry and Food Chemistry, Graz University of Technology, 8010 Graz, Austria*

Ingo Klimant − *Institute of Analytical Chemistry and Food Chemistry, Graz University of Technology, 8010 Graz, Austria*

Complete contact information is available at: https://pubs.acs.org/10.1021/acssensors.9b02512

Author Contributions

[§]S.E.Z. and A.S. contributed equally. All authors have given approval to the final version of the manuscript.

Notes

The authors declare no competing financial interest.

ACKNOWLEDGMENTS

Financial support by the Austrian Academy of Science (ÖAW) at the Institute of Analytical Chemistry and Food Chemistry, Graz University of Technology (DOC-Fellowship #24945 of A.S.), and Austrian Science Fund (project [P32079-N37]) is gratefully acknowledged.

REFERENCES

(1) Borisov, S. M.; Vasylevska, A. S.; Krause, C.; Wolfbeis, O. S. Composite Luminescent Material for Dual Sensing of Oxygen and Temperature. *Adv. Funct. Mater.* **2006**, *16*, 1536−1542.

(2) Zelelow, B.; Khalil, G. E.; Phelan, G.; Carlson, B.; Gouterman, M.; Callis, J. B.; Dalton, L. R. Dual Luminophor Pressure Sensitive Paint. *Sens. Actuators, B* **2003**, *96*, 304−314.

(3) Sung, T.-W.; Lo, Y.-L. Dual Sensing of Temperature and Oxygen Using PtTFPP-Doped CdSe/SiO2 Core−Shell Nanoparticles. *Sens. Actuators, B* **2012**, *173*, 406−413.

(4) Stich, M. I. J.; Nagl, S.; Wolfbeis, O. S.; Henne, U.; Schaeferling, M. A Dual Luminescent Sensor Material for Simultaneous Imaging of Pressure and Temperature on Surfaces. *Adv. Funct. Mater.* **2008**, *18*, 1399−1406.

(5) Köse, M. E.; Carroll, B. F.; Schanze, K. S. Preparation and Spectroscopic Properties of Multiluminophore Luminescent Oxygen and Temperature Sensor Films. *Langmuir* **2005**, *21*, 9121−9129.

(6) Sano, S.; Yuuki, T.; Hyakutake, T.; Morita, K.; Sakaue, H.; Arai, S.; Matsumoto, H.; Michinobu, T. Temperature Compensation of Pressure-Sensitive Luminescent Polymer Sensors. *Sens. Actuators, B* **2018**, *255*, 1960−1966.

(7) Coyle, L. M.; Gouterman, M. Correcting Lifetime Measurements for Temperature. *Sens. Actuators, B* **1999**, *61*, 92−99.

(8) Chu, C.-S.; Lin, T.-H. A New Portable Optical Sensor for Dual Sensing of Temperature and Oxygen. *Sens. Actuators, B* **2014**, *202*, 508−515.

(9) Chu, C.-S.; Lin, T.-H. Ratiometric Optical Sensor for Dual Sensing of Temperature and Oxygen. *Sens. Actuators, B* **2015**, *210*, 302−309.

(10) Collier, B. B.; McShane, M. J. Temperature Compensation of Oxygen Sensing Films Utilizing a Dynamic Dual Lifetime Calculation Technique. *IEEE Sens. J.* **2014**, *14*, 2755−2764.

(11) Köse, M. E.; Omar, A.; Virgin, C. A.; Carroll, B. F.; Schanze, K. S. Principal Component Analysis Calibration Method for Dual-Luminophore Oxygen and Temperature Sensor Films: Application to Luminescence Imaging. *Langmuir* **2005**, *21*, 9110−9120.

(12) Lam, H.; Rao, G.; Loureiro, J.; Tolosa, L. Dual Optical Sensor for Oxygen and Temperature Based on the Combination of Time Domain and Frequency Domain Techniques. *Talanta* **2011**, *84*, 65−70.

(13) Hradil, J.; Davis, C.; Mongey, K.; McDonagh, C.; MacCraith, B. D. Temperature-Corrected Pressure-Sensitive Paint Measurements Using a Single Camera and a Dual-Lifetime Approach. *Meas. Sci. Technol.* **2002**, *13*, 1552−1557.

(14) Lin, F.; Li, F.; Lai, Z.; Cai, Z.; Wang, Y.; Wolfbeis, O. S.; Chen, X. Mn^{II}-Doped Cesium Lead Chloride Perovskite Nanocrystals: Demonstration of Oxygen Sensing Capability Based on Luminescent Dopants and Host-Dopant Energy Transfer. *ACS Appl. Mater. Interfaces* **2018**, *10*, 23335−23343.

(15) Fischer, L. H.; Stich, M. I. J.; Wolfbeis, O. S.; Tian, N.; Holder, E.; Schäferling, M. Red- and Green-Emitting Iridium(III) Complexes for a Dual Barometric and Temperature-Sensitive Paint. *Chem.—Eur. J.* **2009**, *15*, 10857−10863.

(16) Quaranta, M.; Borisov, S. M.; Klimant, I. Indicators for Optical Oxygen Sensors. *Bioanal. Rev.* **2012**, *4*, 115−157.
(17) Wang, X.-d.; Wolfbeis, O. S. Optical Methods for Sensing and Imaging Oxygen: Materials, Spectroscopies and Applications. *Chem. Soc. Rev.* **2014**, *43*, 3666−3761.
(18) Wang, X.-d.; Wolfbeis, O. S.; Meier, R. J. Luminescent Probes and Sensors for Temperature. *Chem. Soc. Rev.* **2013**, *42*, 7834−7869.
(19) Liebsch, G.; Klimant, I.; Wolfbeis, O. S. Luminescence Lifetime Temperature Sensing Based on Sol-Gels and Poly(Acrylonitrile)s Dyed with Ruthenium Metal-Ligand Complexes. *Adv. Mater.* **1999**, *11*, 1296−1299.
(20) Kocincova, A. S.; Borisov, S. M.; Krause, C.; Wolfbeis, O. S. Fiber-Optic Microsensors for Simultaneous Sensing of Oxygen and PH, and of Oxygen and Temperature. *Anal. Chem.* **2007**, *79*, 8486−8493.
(21) Baleizão, C.; Nagl, S.; Schäferling, M.; Berberan-Santos, M. N.; Wolfbeis, O. S. Dual Fluorescence Sensor for Trace Oxygen and Temperature with Unmatched Range and Sensitivity. *Anal. Chem.* **2008**, *80*, 6449−6457.
(22) Fischer, L. H.; Borisov, S. M.; Schaeferling, M.; Klimant, I.; Wolfbeis, O. S. Dual Sensing of PO2 and Temperature Using a Water-Based and Sprayable Fluorescent Paint. *Analyst* **2010**, *135*, 1224.
(23) Karakus, C.; Fischer, L. H.; Schmeding, S.; Hummel, J.; Risch, N.; Schäferling, M.; Holder, E. Oxygen and Temperature Sensitivity of Blue to Green to Yellow Light-Emitting Pt (II) Complexes. *Dalton Trans.* **2012**, *41*, 9623−9632.
(24) Maruszewski, K.; Andrzejewski, D.; Strek, W. Thermal Sensor Based on Luminescence of Ru (Bpy) 32+ Entrapped in Sol-Gel Glasses. *J. Lumin.* **1997**, *72-74*, 226−228.
(25) Fischer, L. H.; Karakus, C.; Meier, R. J.; Risch, N.; Wolfbeis, O. S.; Holder, E.; Schäferling, M. Referenced Dual Pressure- and Temperature-Sensitive Paint for Digital Color Camera Read Out. *Chem.—Eur. J.* **2012**, *18*, 15706−15713.
(26) Khalil, G. E.; Lau, K.; Phelan, G. D.; Carlson, B.; Gouterman, M.; Callis, J. B.; Dalton, L. R. Europium Beta-Diketonate Temperature Sensors: Effects of Ligands, Matrix, and Concentration. *Rev. Sci. Instrum.* **2004**, *75*, 192−206.
(27) Basu, B. B. J.; Vasantharajan, N. Temperature Dependence of the Luminescence Lifetime of a Europium Complex Immobilized in Different Polymer Matrices. *J. Lumin.* **2008**, *128*, 1701−1708.
(28) Basu, B. J.; Venkatraman, S. Fabrication of a Bi-Luminophore Temperature Sensitive Coating by Embedding Europium Thenoyltrifluoroacetonate (EuTTA) and Perylene in Polystyrene. *J. Fluoresc.* **2009**, *19*, 479.
(29) Mitsuishi, M.; Kikuchi, S.; Miyashita, T.; Amao, Y. Characterization of an Ultrathin Polymer Optode and Its Application to Temperature Sensors Based on Luminescent Europium Complexes. *J. Mater. Chem.* **2003**, *13*, 2875−2879.
(30) Borisov, S. M.; Klimant, I. Blue LED Excitable Temperature Sensors Based on a New Europium (III) Chelate. *J. Fluoresc.* **2008**, *18*, 581−589.
(31) Borisov, S. M.; Wolfbeis, O. S. Temperature-Sensitive Europium(III) Probes and Their Use for Simultaneous Luminescent Sensing of Temperature and Oxygen. *Anal. Chem.* **2006**, *78*, 5094−5101.
(32) Sun, L.-N.; Yu, J.; Peng, H.; Zhang, J. Z.; Shi, L.-Y.; Wolfbeis, O. S. Temperature-Sensitive Luminescent Nanoparticles and Films Based on a Terbium (III) Complex Probe. *J. Phys. Chem. C* **2010**, *114*, 12642−12648.
(33) Peng, H.; Stich, M. I. J.; Yu, J.; Sun, L.-n.; Fischer, L. H.; Wolfbeis, O. S. Luminescent Europium(III) Nanoparticles for Sensing and Imaging of Temperature in the Physiological Range. *Adv. Mater.* **2010**, *22*, 716−719.
(34) Peng, H.-S.; Huang, S.-H.; Wolfbeis, O. S. Ratiometric Fluorescent Nanoparticles for Sensing Temperature. *J. Nanoparticle Res.* **2010**, *12*, 2729−2733.
(35) Yu, J.; Sun, L.; Peng, H.; Stich, M. I. J. Luminescent terbium and europium probes for lifetime based sensing of temperature between 0 and 70 °C. *J. Mater. Chem.* **2010**, *20*, 6975−6981.
(36) Wang, X.; Liu, Q.; Bu, Y.; Liu, C.-S.; Liu, T.; Yan, X. Optical Temperature Sensing of Rare-Earth Ion Doped Phosphors. *RSC Adv.* **2015**, *5*, 86219−86236.
(37) Brübach, J.; Pflitsch, C.; Dreizler, A.; Atakan, B. On Surface Temperature Measurements with Thermographic Phosphors: A Review. *Prog. Energy Combust. Sci.* **2013**, *39*, 37−60.
(38) Chen, Z.; Zhang, K. Y.; Tong, X.; Liu, Y.; Hu, C.; Liu, S.; Yu, Q.; Zhao, Q.; Huang, W. Phosphorescent Polymeric Thermometers for In Vitro and In Vivo Temperature Sensing with Minimized Background Interference. *Adv. Funct. Mater.* **2016**, *26*, 4386−4396.
(39) Okabe, K.; Inada, N.; Gota, C.; Harada, Y.; Funatsu, T.; Uchiyama, S. Intracellular Temperature Mapping with a Fluorescent Polymeric Thermometer and Fluorescence Lifetime Imaging Microscopy. *Nat. Commun.* **2012**, *3*, 705−713.
(40) Albers, A. E.; Chan, E. M.; McBride, P. M.; Ajo-Franklin, C. M.; Cohen, B. E.; Helms, B. A. Dual-Emitting Quantum Dot/Quantum Rod-Based Nanothermometers with Enhanced Response and Sensitivity in Live Cells. *J. Am. Chem. Soc.* **2012**, *134*, 9565−9568.
(41) Yang, J.-M.; Yang, H.; Lin, L. Quantum Dot Nano Thermometers Reveal Heterogeneous Local Thermogenesis in Living Cells. *ACS Nano* **2011**, *5*, 5067−5071.
(42) Park, Y.; Koo, C.; Chen, H.-Y.; Han, A.; Son, D. H. Ratiometric Temperature Imaging Using Environment-Insensitive Luminescence of Mn-Doped Core−Shell Nanocrystals. *Nanoscale* **2013**, *5*, 4944−4950.
(43) Liang, R.; Tian, R.; Shi, W.; Liu, Z.; Yan, D.; Wei, M.; Evans, D. G.; Duan, X. A Temperature Sensor Based on CdTe Quantum Dots−Layered Double Hydroxide Ultrathin Films via Layer-by-Layer Assembly. *Chem. Commun.* **2013**, *49*, 969−971.
(44) Haro-González, P.; Martínez-Maestro, L.; Martín, I. R.; García-Solé, J.; Jaque, D. High-Sensitivity Fluorescence Lifetime Thermal Sensing Based on CdTe Quantum Dots. *Small* **2012**, *8*, 2652−2658.
(45) Hsia, C.-H.; Wuttig, A.; Yang, H. An Accessible Approach to Preparing Water-Soluble Mn2+-Doped (CdSSe) ZnS (Core) Shell Nanocrystals for Ratiometric Temperature Sensing. *ACS Nano* **2011**, *5*, 9511−9522.
(46) McLaurin, E. J.; Vlaskin, V. A.; Gamelin, D. R. Water-Soluble Dual-Emitting Nanocrystals for Ratiometric Optical Thermometry. *J. Am. Chem. Soc.* **2011**, *133*, 14978−14980.
(47) Donner, J. S.; Thompson, S. A.; Kreuzer, M. P.; Baffou, G.; Quidant, R. Mapping Intracellular Temperature Using Green Fluorescent Protein. *Nano Lett.* **2012**, *12*, 2107−2111.
(48) Fister, J. C.; Rank, D.; Harris, J. M. Delayed Fluorescence Optical Thermometry. *Anal. Chem.* **1995**, *67*, 4269−4275.
(49) Baleizão, C.; Nagl, S.; Borisov, S. M.; Schäferling, M.; Wolfbeis, O. S.; Berberan-Santos, M. N. An Optical Thermometer Based on the Delayed Fluorescence of C70. *Chem.—Eur. J.* **2007**, *13*, 3643−3651.
(50) Jenkins, J.; Borisov, S. M.; Papkovsky, D. B.; Dmitriev, R. I. Sulforhodamine Nanothermometer for Multiparametric Fluorescence Lifetime Imaging Microscopy. *Anal. Chem.* **2016**, *88*, 10566−10572.
(51) Baker, G. A.; Baker, S. N.; McCleskey, T. M. Noncontact Two-Color Luminescence Thermometry Based on Intramolecular Luminophore Cyclization within an Ionic Liquid. *Chem. Commun.* **2003**, 2932−2933.
(52) Cao, C.; Liu, X.; Qiao, Q.; Zhao, M.; Yin, W.; Mao, D.; Zhang, H.; Xu, Z. A Twisted-Intramolecular-Charge-Transfer (TICT) Based Ratiometric Fluorescent Thermometer with a Mega-Stokes Shift and a Positive Temperature Coefficient. *Chem. Commun.* **2014**, *50*, 15811−15814.
(53) Ross, D.; Gaitan, M.; Locascio, L. E. Temperature Measurement in Microfluidic Systems Using a Temperature-Dependent Fluorescent Dye. *Anal. Chem.* **2001**, *73*, 4117−4123.
(54) Duong, H. D.; Rhee, J. I. Exploitation of Thermo-Effect of Rhodamine B Entrapped in Sol−Gel Matrix and Silica Gel for Temperature Detection. *Sens. Actuators, B* **2007**, *124*, 18−23.
(55) Jorge, P. A. S.; Maule, C.; Silva, A. J.; Benrashid, R.; Santos, J. L.; Farahi, F. Dual Sensing of Oxygen and Temperature Using Quantum Dots and a Ruthenium Complex. *Anal. Chim. Acta* **2008**, *606*, 223−229.

https://dx.doi.org/10.1021/acssensors.9b02512
ACS Sens. 2020, 5, 1020−1027

(56) Steinegger, A.; Klimant, I.; Borisov, S. M. Purely Organic Dyes with Thermally Activated Delayed Fluorescence-A Versatile Class of Indicators for Optical Temperature Sensing. *Adv. Opt. Mater.* **2017**, *5*, 1700372.
(57) Zach, P. W.; Freunberger, S. A.; Klimant, I.; Borisov, S. M. Electron-Deficient Near-Infrared Pt(II) and Pd(II) Benzoporphyrins with Dual Phosphorescence and Unusually Efficient Thermally Activated Delayed Fluorescence: First Demonstration of Simultaneous Oxygen and Temperature Sensing with a Single Emitter. *ACS Appl. Mater. Interfaces* **2017**, *9*, 38008−38023.
(58) Wong, M. Y.; Zysman-Colman, E. Purely Organic Thermally Activated Delayed Fluorescence Materials for Organic Light-Emitting Diodes. *Adv. Mater.* **2017**, *29*, 1605444.
(59) Yang, Z.; Mao, Z.; Xie, Z.; Zhang, Y.; Liu, S.; Zhao, J.; Xu, J.; Chi, Z.; Aldred, M. P. Recent Advances in Organic Thermally Activated Delayed Fluorescence Materials. *Chem. Soc. Rev.* **2017**, *46*, 915−1016.
(60) Tao, Y.; Yuan, K.; Chen, T.; Xu, P.; Li, H.; Chen, R.; Zheng, C.; Zhang, L.; Huang, W. Thermally Activated Delayed Fluorescence Materials Towards the Breakthrough of Organoelectronics. *Adv. Mater.* **2014**, *26*, 7931−7958.
(61) Borisov, S. M.; Neurauter, G.; Schroeder, C.; Klimant, I.; Wolfbeis, O. S. Modified Dual Lifetime Referencing Method for Simultaneous Optical Determination and Sensing of Two Analytes. *Appl. Spectrosc.* **2006**, *60*, 1167−1173.
(62) Larndorfer, C.; Borisov, S. M.; Lehner, P.; Klimant, I. The Effect of High Light Intensities on Luminescence Lifetime Based Oxygen Sensing. *Analyst* **2014**, *139*, 6569−6579.
(63) Stehning, C.; Holst, G. A. Addressing Multiple Indicators on a Single Optical Fiber—Digital Signal Processing Approaches for Temperature Compensated Oxygen Sensing. *IEEE Sens. J.* **2004**, *4*, 153−159.
(64) Carraway, E. R.; Demas, J. N.; DeGraff, B. A. Luminescence Quenching Mechanism for Microheterogeneous Systems. *Anal. Chem.* **1991**, *63*, 332−336.
(65) Carraway, E. R.; Demas, J. N.; DeGraff, B. A.; Bacon, J. R. Photophysics and Photochemistry of Oxygen Sensors Based on Luminescent Transition-Metal Complexes. *Anal. Chem.* **1991**, *63*, 337−342.
(66) *Polymer Handbook*, 4th ed.; Brandrup, J., Immergut, E. H., Grulke, E. A., Eds.; Wiley: New York, Chichester, 2004.

https://dx.doi.org/10.1021/acssensors.9b02512
ACS Sens. 2020, 5, 1020−1027